Micro-Raman and Luminescence Spectroscopic Techniques for the Characterization and Process Control of Rb^+ Exchanged $KTiOPO_4$ Waveguides

David D. Tuschel[1], Suzanne D. Lau[2], and William P. Risk[3]

[1]Imaging Research and Advanced Development
Eastman Kodak Company
Research Laboratories
Rochester, NY 14650-2017

[2]Uniphase
163 Baypointe Parkway
San Jose, CA 95134

[3]IBM Research Division
Almaden Research Center
650 Harry Rd.
San Jose, CA 95120

ABSTRACT

The fabrication of ion-exchanged waveguides with high-frequency doubling conversion efficiency requires high-quality crystalline substrates, an understanding of the effects of partial cation exchange on the optical properties of the waveguide, and control of the degree and effects of ion-exchange. To address these needs we have developed micro-Raman and luminescence spectroscopic techniques for the characterization and process control of Rb^+ exchanged $KTiOPO_4$ (R/KTP) waveguides. We report on the use of laser excited luminescence to screen device substrates for unacceptable levels of impurity transition metals, which contribute to photorefraction and optical losses due to absorption. Micro-Raman spectroscopy has been used to probe tops of R/KTP channel waveguides for the degree and effects of Rb^+ exchange. The high spatial resolution and nondestructive nature of micro-Raman spectroscopy make it suitable as a probe for *in situ* characterization of photonic devices. Specifically, micro-Raman spectroscopy can detect cation-exchange induced changes in the polarizability, reduction of crystal symmetry, and changes in the chemical bonding and orientation of the TiO_6 octahedra, the anionic groups primarily responsible for the nonlinear properties of the material. Individual R/KTP waveguides from different devices have been studied by micro-Raman spectroscopy and structural differences have been detected. The uniformity of a channel waveguide is another quality that can be readily probed and quantified by micro-Raman spectroscopy.

Keywords: Raman spectroscopy, luminescence, potassium titanyl phosphate, channel waveguide, ion-exchange

1. INTRODUCTION

A compact blue laser would be highly desirable for optical data storage. Commercially available optical storage devices rely on III-V semiconductor lasers operating at near infrared wavelengths. Greater information density could be achieved by using a shorter wavelength laser which would have a smaller diffraction limit. One approach to building a compact blue laser is based upon second harmonic generation. Near infrared radiation from a semiconductor laser is endfired into a waveguide fabricated from a material such as $KTiOPO_4$ (KTP), which has a high nonlinear susceptibility. Partial ion-exchange of the alkali cation in single-crystal transition metal oxides that manifest a high optical nonlinearity is a convenient way of fabricating waveguides for second harmonic generation.[1-4] Structural characterizations of the products of partial

cation-exchange reactions involving titanyl phosphates have been performed.[5-12] However, there is only a limited understanding of how ion-exchange affects the chemical and crystal structure and concomitantly the refractive index and the nonlinear susceptibility. Although much work has been done on powders to understand the the structural changes brought about by ion-exchange, there have been only a few reported studies on the chemical and crystal structure of Rb^+ exchanged $KTiOPO_4$ (R/KTP) waveguides.[13-16] Understanding and controlling the relationship of structure to property would guide researchers in establishing those fabrication conditions that produce waveguides with optimal performance. The primary purpose of this work is to demonstrate that structural differences between R/KTP channel waveguides can be detected by micro-Raman spectroscopy. Secondly, we want to establish nondestructive, microspectroscopic methods for the evaluation of waveguide substrates and for the process control of R/KTP waveguide fabrication.

The quality of the crystal prior to waveguide fabrication can have a significant effect on the performance of the device. Optical damage to crystalline inorganic waveguides has often been attributed to intrinsic contaminants in the form of transition metal ions. Fe, Cu, Cr and Mn are contaminant metals known to be present in metal oxide crystals at parts per million levels or less. We have performed laser excited luminescence studies to determine if the contaminant metal level is dependent upon the method of KTP growth. Furthermore, we wish to identify the contaminant metal ions that are optically active in KTP, their relative amounts, and their effect on the structure and optical properties of the host lattice.

2. EXPERIMENTAL CONDITIONS

Patterns for segmented waveguides positioned parallel to the Y axis were established by depositing an Al mask on the Z-face of a KTP crystal. Channel waveguides were subsequently fabricated by carrying out a partial ion-exchange of K^+ in a melt containing $RbNO_3$ (92% molar) and $Ba(NO_3)_2$ (8%). The ion-exchange for all but one of the devices was carried out at 375° C for 10 minutes. The reaction for device 941123.12 was carried out at 375° C for 5 minutes. The micro-Raman study was performed by focussing a X-polarized, ~15 mW, 488.0 nm laser beam (0.6 μm diameter) with an Olympus MS Plan 100 (0.95 NA) objective at various positions on the Z-face of the device. The same microscope objective is used to collect backscattered light, which was guided into an Instruments SA S3000 spectrometer with slits at 200 μm/~3.5 mm/200 μm. A pinhole aperture was positioned in front of the spectrometer entrance slit to enhance axial spatial resolution. The aperture is essential for excluding the signal from the substrate KTP when probing the shallow R/KTP waveguides from the top. Micro-Raman spectra were detected using an EEV Class One #15-11 CCD. No polarization analyzer was used. The Porto notation for the micro-Raman experiments reported here is $Z(X,XY)\bar{Z}$, where the first and second symbols outside the parenthesis correspond to the excitation and scattering propagation directions, respectively. The first and second symbols within the parenthesis denote the excitation and scattering polarizations, respectively.

KTP crystals were probed for transition metal impurities using laser excited luminescence. Bulk contamination was probed by performing the work in the macro arrangement. Our primary excitation was 235 mW of 457.9 nm light. However, we did use 488.0 nm and 647.1 nm light to test the breadth of the excitation manifold. The slits were set to 400 μm/400 μm/400 μm/400 μm and scans were made from 21,638.8 cm^{-1} to 11,843.8 cm^{-1} in 15.0 cm^{-1} increments at 1.0 s integration time. Luminescence spectra were detected with a Hamamatsu R943-02 photomultiplier tube. Spectra were collected either by focussing the beam on the Z-face of the crystal, the Z-axis and incident beam forming approximately a 45° angle, or the beam was guided parallel to the Y-axis and incident upon the Y-face of the crystal. The emitted light was collected at 90° with respect to the incident beam, and no polarization analyzer was used.

3. DISCUSSION OF RESULTS

The primary advantages of micro-Raman spectroscopy as applied to the characterization of photonic devices are its high spatial (lateral and axial) resolution and that reference spectra are obtained directly from the device being probed. Therefore, absent physical defects such as surface roughness, differences in micro-

Raman spectra obtained from different locations on the device can be interpreted in terms of chemical and crystal structure. Such changes, induced by the ion-exchange reaction, can be seen in the micro-Raman spectra of the KTP substrate and the last segment of a channel waveguide from device U941123.14 shown in Fig. 1. The spectra were obtained under identical conditions; i.e., the beam was easily positioned by moving the device on a microscope translation stage. Consequently, the differences in band positions and relative intensities can be attributed to structural changes induced by the partial cation-exchange. The Raman spectrum obtained from any face of a KTP crystal consists primarily of bands due to the vibrational motions of the TiO_6 octahedra and the PO_4 tetrahedra.[17] Raman bands below 200 cm^{-1} are assigned to alkali cation translational modes, and therefore manifest the most significant changes subsequent to Rb^+ exchange. Bands in the 200-400 cm^{-1} and 600-850 cm^{-1} region are attributed to TiO_6 octahedral torsional and stretching modes, respectively. Not shown here are the bands in the 900-1200 cm^{-1} region associated with the PO_4 tetrahedra. In an earlier work, we showed that the spectral changes observed in conjunction with Rb^+ exchange are similar to those for a directional dispersion; i.e., the strength and frequency of Raman bands are dependent upon the direction of phonon propagation.[6] We explained our results in terms of a Rb^+ exchange mechanism that, because of the relatively larger ionic radius of Rb^+ (r_{Rb} = 1.49 Å, r_K = 1.33 Å), causes a reorientation or tilting of the octahedra to accommodate the larger cation. Consequently, the spectral changes observed with Rb^+ exchange are similar to those of a directional dispersion. It is the sensitivity of micro-Raman spectroscopy to such changes in chemical bonding and crystal structure that makes it suitable for monitoring the fabrication of R/KTP waveguides.

The KTP spectra shown in Figs. 2 and 3 illustrate how micro-Raman spectroscopy can be used to probe the structural (chemical and crystal) changes induced by Rb^+ exchange. The cation translational mode portion of the KTP substrate spectra shown in Fig. 2 were obtained from 5 R/KTP channel waveguide devices. All 5 devices were positioned together on the micro-Raman stage such that their waveguides were parallel. The KTP substrates and R/KTP waveguide segments were then analyzed during the same session. The spectra are plotted normalized to the 121 cm^{-1} band to remove spectral differences due to background scattering from surface roughness. The spectra match extremely well, and show only minor differences in the shoulder at 124 cm^{-1} and the band at 153 cm^{-1}. In contrast, the corresponding spectra of R/KTP segments in Fig. 3 show significant differences in relative scattering strength and in band shape, particularly the 165 cm^{-1} band. Four of the five devices were fabricated under identical conditions. One device was limited to one-half the ion-exchange time as the other four devices; however, its Raman spectrum falls within the distribution of all five spectra, thereby suggesting that its structure near the surface is not significantly different from the near-surface structure of the other four. The spectra of the KTP substrates in Fig. 2 indicate that the precision of the micro-Raman measurement is sufficient to detect structural differences in R/KTP channel waveguide devices, even those that are nominally the same.

The R/KTP segments discussed above were selected at random from the interior of the devices and were representative of most of the waveguide. We have found that segments near the ends of the device can be structurally quite different from the majority of the waveguide. The structural differences are clear from the micro-Raman spectra and from the contrast observed when viewed under crossed polarization with an optical microscope. When viewing the Z-face of an R/KTP waveguide device with X-polarized transmitted light and the analyzer Y-polarized, most of the device appears dark. However, many of the end segments and the corners of test patterns appear bright, presumably due to stress birefringence. It is clear from the varying brightness of the end segments that there is an associated structural variance. Micro-Raman spectra of the end segments of three adjacent waveguides are shown in Fig. 4; they confirm the structural variance observed under crossed polarization. The spectra are plotted normalized to the 216 cm^{-1} band to show the changes in relative band strength, and therefore the structural differences, in the end segments of adjacent waveguides. Micro-Raman spectra confirm that the light leakage corresponds to localized strain in the crystal. Specifically, the end segments of waveguides 57, 56, and 55 appear progressively brighter, and the corresponding micro-Raman spectra show a progressive deviation from the reference spectrum of the KTP substrate. At this time we cannot correlate end segment structure to the performance of the waveguide. However, in future work we will try to determine if strain in the end segment, as observed by polarized light microscopy and micro-Raman spectroscopy, can be correlated to the waveguide coupling efficiency.

The uniformity of an R/KTP channel waveguide is another quality that can be readily probed and quantified by micro-Raman spectroscopy. Referring to Fig. 1, note the dramatic change in the strength of the band at 340 cm^{-1} relative to that at 373 cm^{-1}. (The band positions noted in Fig. 1 are for R/KTP and are dependent upon the degree of Rb^+ exchange. For simplicity we refer to the KTP band positions when quantifying the relative strengths of R/KTP bands.) A plot of S_{342}/S_{375} as a function of waveguide segment number, as shown in Fig. 5, reveals the structural variation in waveguide 55 from device U941123.14. The mean value of S_{342}/S_{375} is 0.862 ± 0.017. The S_{342}/S_{375} of segment No. 1 was excluded from the determination of the mean because the end segments are not representative of the majority of the waveguide. A set of reference spectra from KTP substrate adjacent to the waveguides were also collected. The KTP mean value of S_{342}/S_{375} is 1.14 ± 0.01. Measuring the relative strengths of Raman bands is a sensitive and convenient way to compare the degree and effects of Rb^+ exchange in different devices and the variability of a single waveguide. Determining relative band strengths avoids the problem of comparing absolute signal strengths from different devices. Furthermore, the reference KTP spectra are generated from the device, and so the differences between S_{342}/S_{375} from KTP and R/KTP waveguides must be entirely due to structural differences in R/KTP.

It was found that laser excited luminescence could be generated by every flux-grown KTP crystal. The emission spectrum consisted of a broad band centered at ~790 nm with a narrower sideband at 837 nm. That the same emission spectrum could be obtained from crystals provided by different crystal growers suggests that contamination with this chromophore is specific to the flux-growth method. The presence of optically active contaminants in flux-grown KTP will contribute to losses by absorption of the frequency doubled light. Also, metal contaminants could contribute to photorefractive damage. A cursory review of the literature suggests that the chromophore responsible for the luminescence could be iron or chromium ions.[18] To identify the metal contaminants, and the chromophore, present in KTP we have had neutron activation analysis performed on the KTP crystal from Brimrose. Fe (<20.8 ppm) and Cr (3.9 ppm) were detected along with Ni (<9.9 ppm) and Zn (4.2 ppm). Therefore, we do not yet know whether iron or chromium is responsible for the luminescence in flux-grown KTP.

The hydrothermally-grown (HT) KTP samples, with the single exception of S1.3, did not luminesce. The S1.3 emission spectrum consisted of a broad band centered at ~545 nm, clearly due to a different chromophore from that observed in the flux-grown crystals. The results of the luminescence study are tabulated below. We plan to obtain visible absorption spectra of flux- and hydrothermally-grown crystals to identify the chromophores present in each and to compare the relative optical losses of crystals. Also, we will obtain absorption spectra of optically damaged (gray track) KTP to understand the role that impurities play in gray tracking.

Table 1: Laser Excited (457.9, 488.0, and 647.1 nm) Emission Bands from KTP

Sample	λ_{max} (nm)	Growth Type
S1.3	545	HT
U941123.14	None	HT
U941123.12	None	HT
U940216.1	None	HT
IBM 1058-1B-1	None	HT
KTP F11	~800 (837)	Flux
KTP F16 (b)	~790 (837)	Flux
IBM R/KTP	~790 (837)	Flux
Brimrose	~790 (837)	?
U950530.16	~790 (837)	Flux
IBM A1	~790 (837)	Flux
IBM A4	~790 (837)	Flux
IBM B2	~790 (837)	Flux
Casix	~790 (837)	Flux

4. CONCLUSIONS

The primary advantages of micro-Raman spectroscopy as applied to the characterization of photonic devices are its high spatial (lateral and axial) resolution and that reference spectra are obtained directly from the device being probed. Therefore, absent physical defects such as surface roughness, differences in micro-Raman spectra obtained from different locations on the device can be interpreted in terms of chemical and crystal structure. Such stress-induced birefringence was observed at waveguide endfaces and at the corners of test patterns in R/KTP devices. Light leakage due to stress can be observed by viewing the Z-face of the device under crossed polarization with X-polarized transmitted light. Micro-Raman spectra confirm that the light leakage corresponds to localized strain in the crystal. Specifically, the end segments of adjacent waveguides which appear progressively brighter yield micro-Raman spectra which also deviate correspondingly from the reference spectrum of the KTP substrate. Measuring the relative strengths of Raman bands is a sensitive and convenient way to compare the degree and effects of Rb^+ exchange in different devices and the variability of a single waveguide. Determining relative band strengths avoids the problem of comparing absolute signal strengths from different devices. Furthermore, the reference KTP spectra are generated from the device, and so the differences between S_{342}/S_{375} from KTP and R/KTP waveguides must be entirely due to structural differences in R/KTP. Finally, it was found that laser excited luminescence could be generated by every flux-grown KTP crystal. That the same emission spectrum could be obtained from crystals provided by different crystal growers suggests that contamination with this chromophore is specific to the flux-growth method.

5. ACKNOWLEDGEMENTS

We would like to acknowledge Albert Filo of Eastman Kodak for performing the neutron activation analysis. Also, we would like to thank John Agostinelli and James Chwalek of Eastman Kodak for helpful discussions.

6. REFERENCES

1. J. D. Bierlein, A. Ferretti, L. H. Brixner, and W. Y. Hsu, "Fabrication and characterization of optical waveguides in $KTiOPO_4$," *Appl. Phys. Lett.* **50**, 1216-1218 (1987).
2. J. D. Bierlein, D. B. Laubacher, J. B. Brown, and C. J. van der Poel, "Balanced phase matching in segmented $KTiOPO_4$ waveguides," *Appl. Phys. Lett.* **56**, 1725-1727 (1990).
3. W. P. Risk, "Fabrication and characterization of planar ion-exchanged $KTiOPO_4$ waveguides for frequency doubling," *Appl. Phys. Lett.* **58**, 19-21 (1991).
4. M. E. Hagerman and K. R. Poeppelmeier, "Review of the structure and processing-defect-property relationships of potassium titanyl phosphate: A strategy for novel thin-film photonic devices," *Chem. Mater.* **7**, 602-621 (1995).
5. M. L. Phillips, T. E. Gier, M. M. Eddy, N. L. Keder, G. D. Stucky, and J. D. Bierlein, "Inclusion tuning of nonlinear optical materials: KTP isomorphs," *Sol. State Ionics* **32/33**, 147-153 (1989).
6. M. L. F. Phillips, W. T. A. Harrison, T. E. Gier, G. D. Stucky, G. V. Kulkarni, J. K. Burdett, "Electronic effects of substitution chemistry in the $KTiOPO_4$ structure field: Structure and optical properties of potassium vanadyl phosphate," *Inorg. Chem.* **29**, 2158-2163 (1990).
7. G. D. Stucky, M. L. F. Phillips, T. E. Gier, "The potassium titanyl phosphate structure field: A model for new nonlinear optical materials," *Chem. Mater.* **1**, 492-509 (1989).
8. M. L. F. Phillips, W. T. A. Harrison, G. D. Stucky, E. M. McCarron III, J. C. Calabrese, and T. E. Gier, "Effects of substitution chemistry in the $KTiOPO_4$ structure field," *Chem. Mater.* **4**, 222-233 (1992).

9. S. J. Crennell, R. E. Morris, A. K. Cheetham, and R. H. Jarman, "Isomorphous substitution in $KTiOPO_4$: A single-crystal diffraction study of members of the $K_{1-x}Na_xTiOPO_4$ solid solution," *Chem. Mater.* **4**, 82-88 (1992).
10. P. A. Thomas, S. C. Mayo and B. E. Watts, "Crystal structures of $RbTiOAsO_4$, $KTiO(P_{0.58},As_{0.42})O_4$, $RbTiOPO_4$ and $(Rb_{0.465},K_{0.535})TiOPO_4$, and analysis of pseudosymmetry in crystals of the $KTiOPO_4$ family," *Acta Cryst.* **B48**, 401-407 (1992).
11. G. M. Loiacono, R. A. Stolzenberger and D. N. Loiacono, "Modified $KTiOPO_4$ crystals for noncritical phase matching applications," *Appl. Phys. Lett.* **64**, 16-18 (1994).
12. M. L. F. Phillips, W. T. A. Harrison, and G. D. Stucky, "Comment on: 'Modified $KTiOPO_4$ crystals for noncritical phase matching applications' [Appl. Phys. Lett. 64, 16 (1994)]," *Appl. Phys. Lett.* **66**, 3070-3071 (1995).
13. D. D. Tuschel, G. R. Paz-Pujalt, and W. P. Risk, "Chemical bonding and atomic structure of Rb^+ exchanged $KTiOPO_4$ waveguides probed by micro-Raman spectroscopy," *Appl. Phys. Lett.* **66**, 1035-1037 (1995).
14. I. Savatinova, S. Tonchev, T. Popov, E. Liarokapis, and C. C. Ziling, "Raman study of Cs:$KTiOPO_4$ waveguides," *J. Phys. D: Appl. Phys.* **27**, 1384-1389 (1994).
15. C. L. Jahncke, M. A. Paesler, and H. D. Hallen, "Raman imaging with near-field scanning optical microscopy," *Appl. Phys. Lett.* **67**, 2483-2485 (1995).
16. A. A. Lipovskii, N. V. Nikonorov, and V. A. Lokalov, "Study of optically waveguiding structures formed in potassium titanyl phosphate by ion exchange," **33**, 2632-2637 (1994).
17. G. E. Kugel, F. Bréhat, B. Wyncke, M. D. Fontana, G. Marnier, C. Carabatos-Nedelec, and J. Mangin, "The vibrational spectrum of a $KTiOPO_4$ single crystal studied by Raman and infrared reflectivity spectroscopy," *J. Phys. C: Solid State Phys.* **21**, 5565-5583 (1988).
18. P. A. Morris, "Chapter 25: Defect chemistry of nonlinear optical oxide crystals," *Materials for Nonlinear Optics: Chemical Perspectives*, edited by S. R. Marder, J. E. Sohn and G. D. Stucky, 380-393 (American Chemical Society, Washington, D.C., 1991).

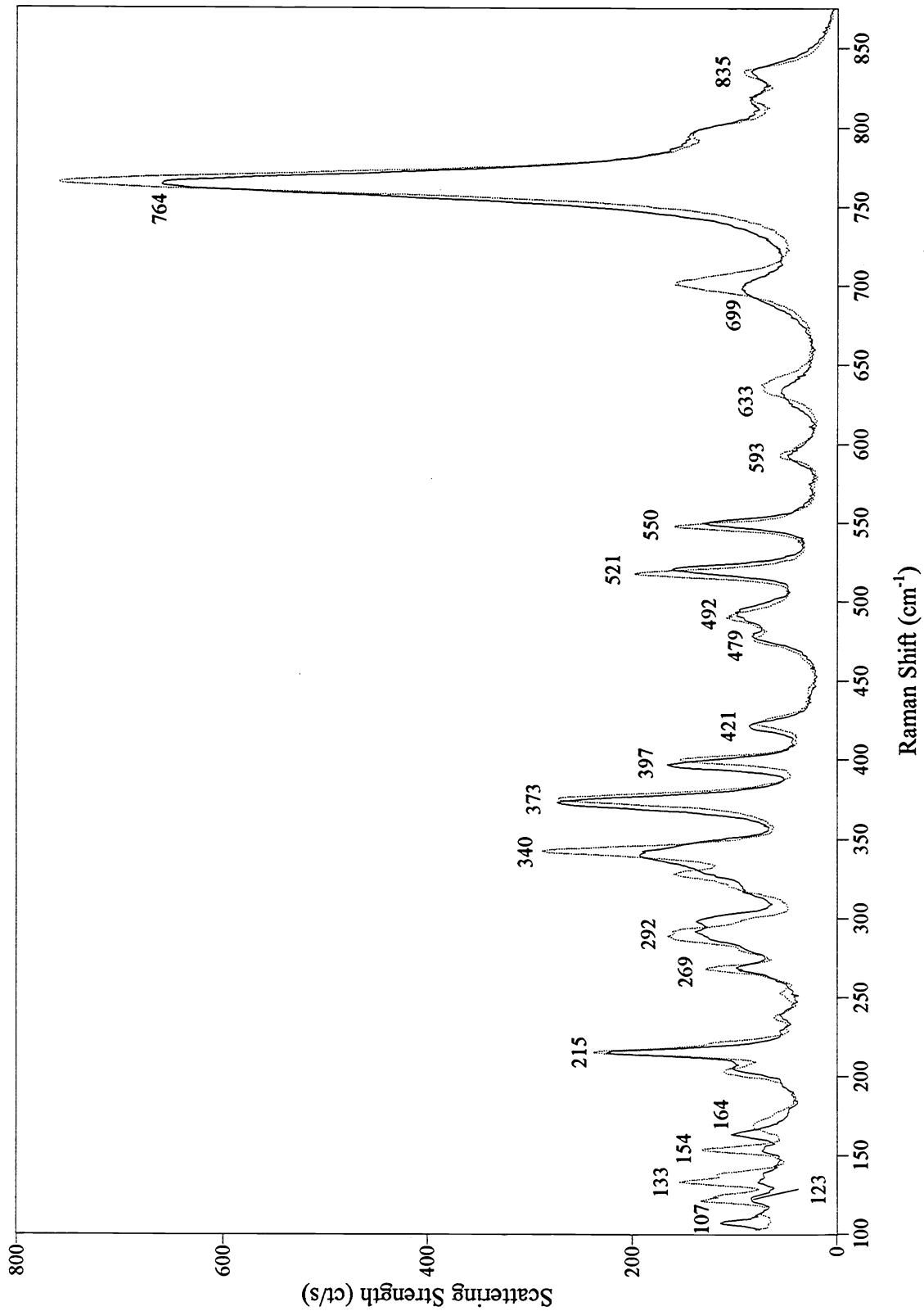

Fig. 1. Micro-Raman spectra of the last segment of R/KTP channel waveguide 55 from device U941123.14 (solid) and the KTP substrate (dotted). Spectra were obtained from the Z face and the excitation was X-polarized. Band positions are for the R/KTP waveguide spectrum.

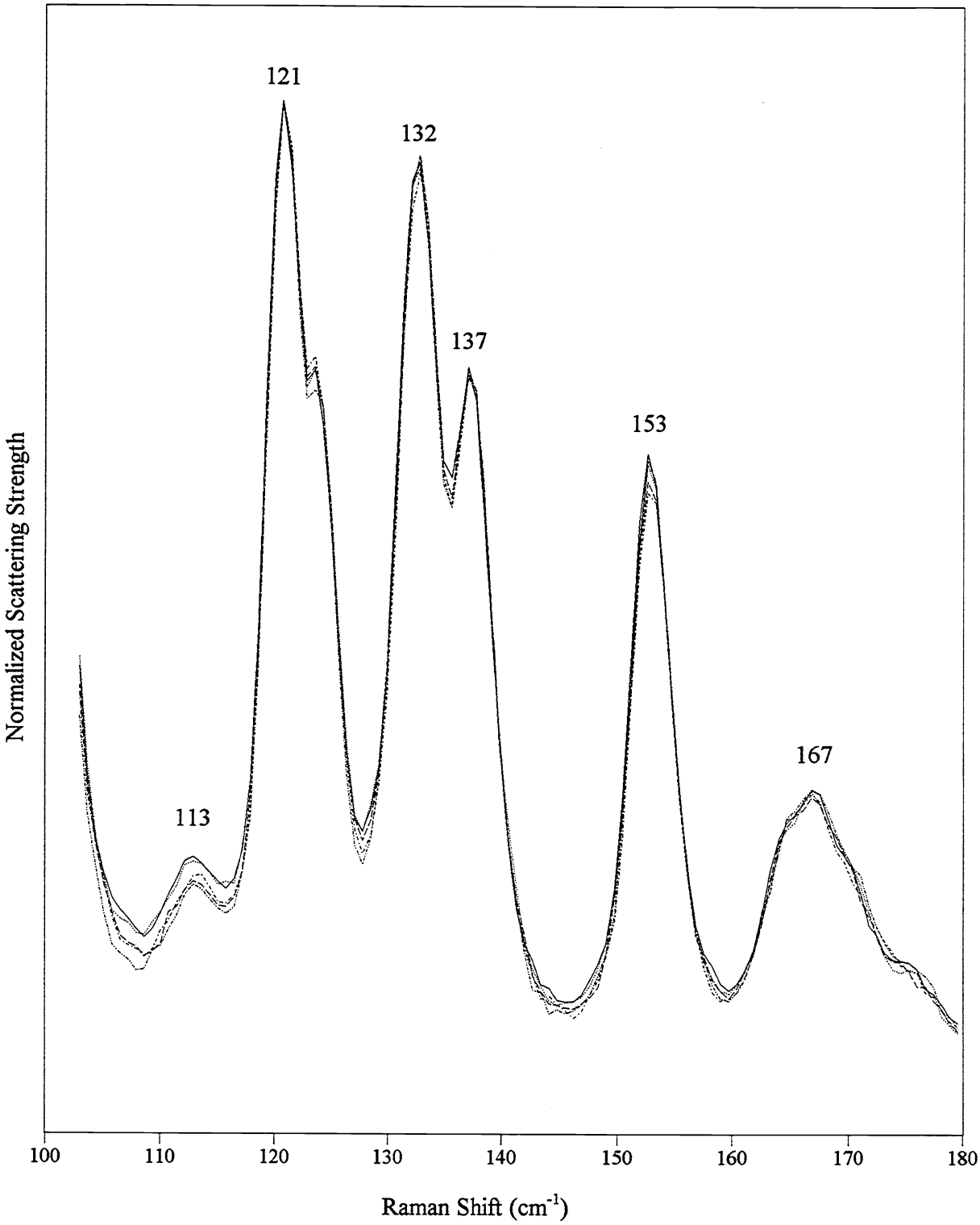

Fig. 2. Micro-Raman spectra of the KTP substrates from R/KTP channel waveguide devices Casix 940621.1 (solid), CTI 940614.11 (dotted), U941123.14 (dashed), U941123.12 (dash dot), and S1.3 (dash dot dot).

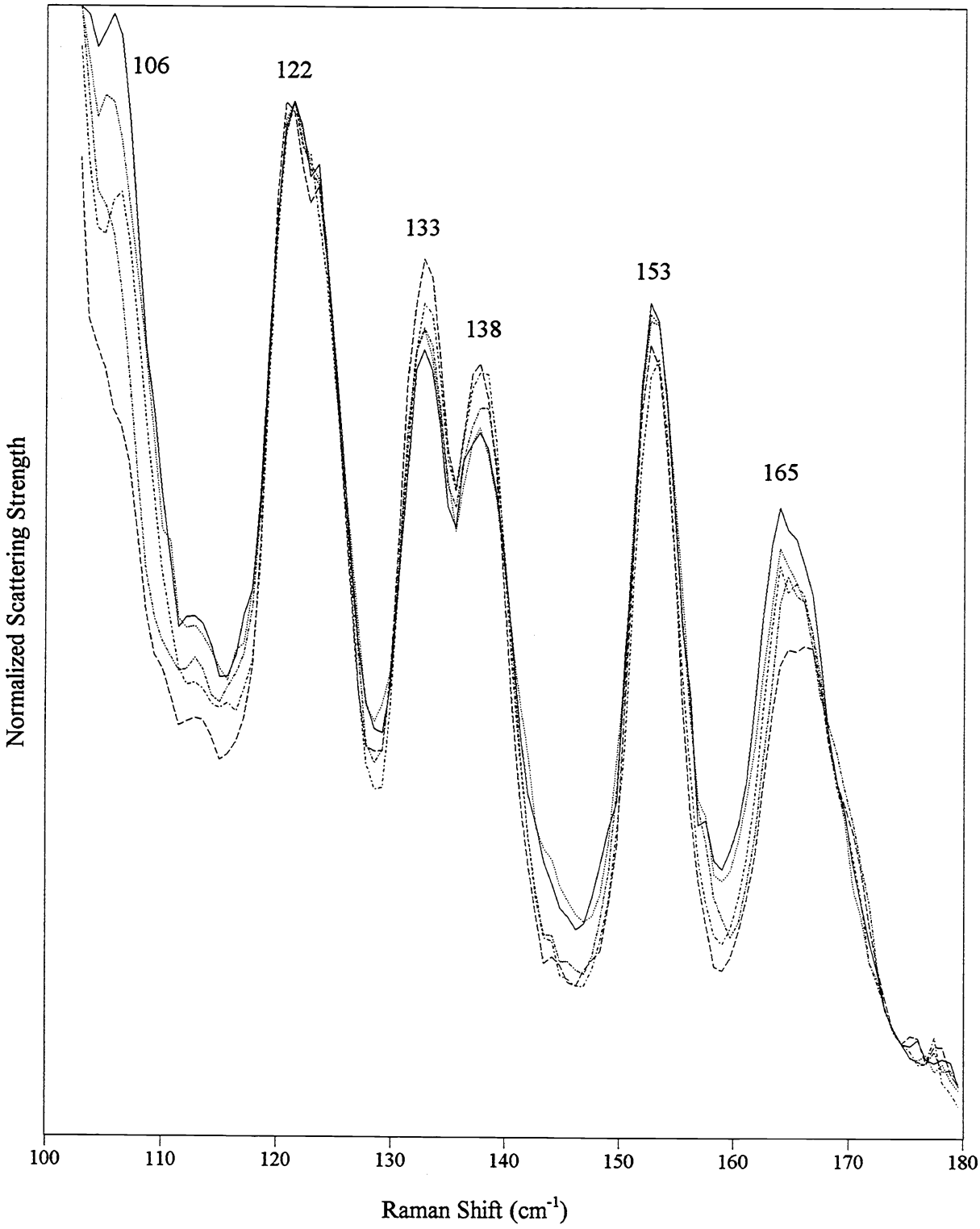

Fig. 3. Micro-Raman spectra of interior segments of R/KTP channel waveguides from devices Casix 940621.1 (solid), CTI 940614.11 (dotted), U941123.14 (dashed), U941123.12 (dash dot), and S1.3 (dash dot dot).

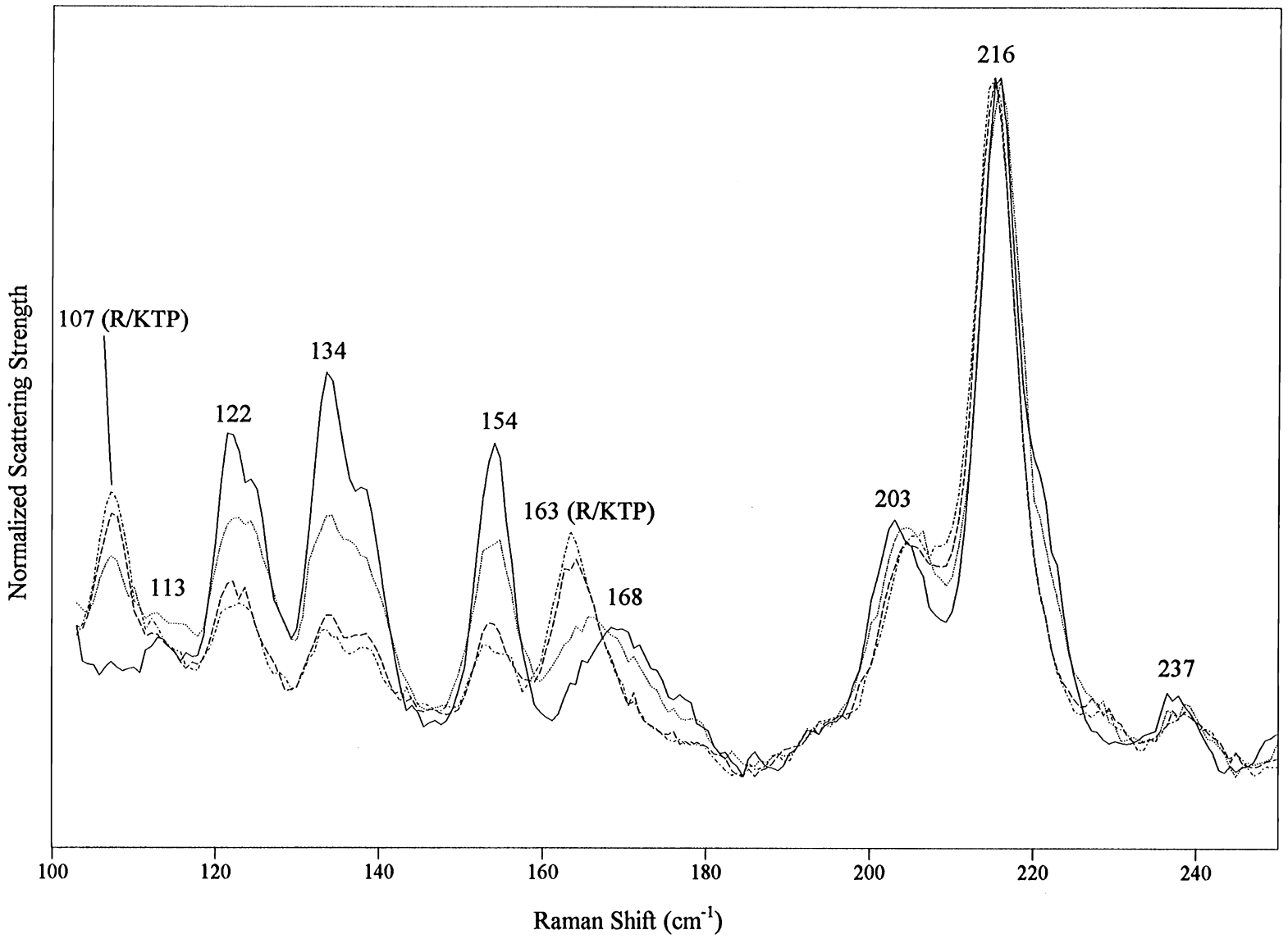

Fig. 4. Micro-Raman spectra of the KTP substrate (solid) and the last segments of R/KTP channel waveguides 57 (dotted), 56 (dashed), 55 (dash dot) from device U941123.14. Spectra have been normalized to the 216 cm^{-1} band to show the changes in relative band strength, and therefore the structural differences, in the end segments of adjacent waveguides. Band positions are for the KTP substrate spectrum; those labeled R/KTP are for waveguide 55.

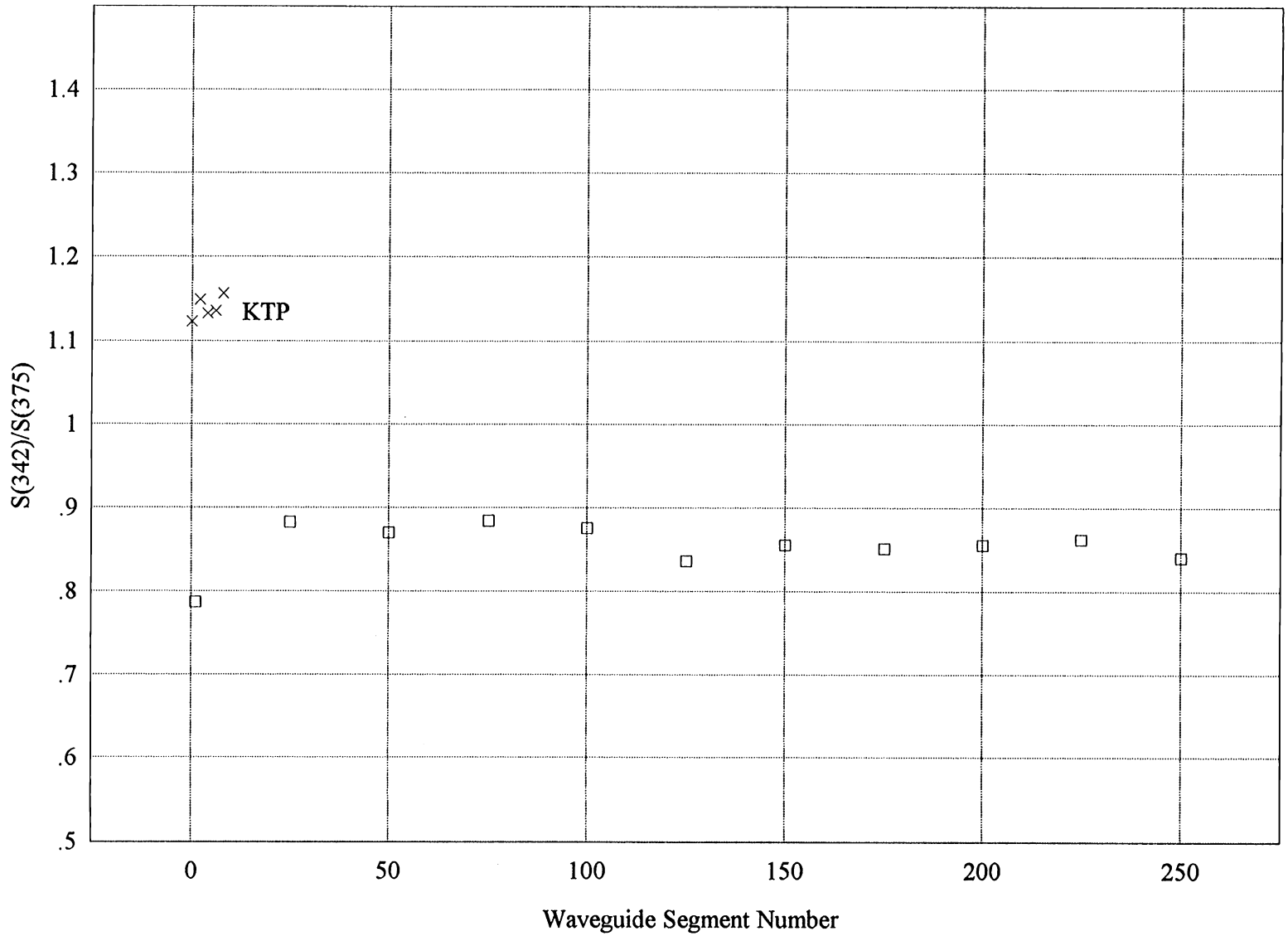

Fig. 5. Strengths of the 342 cm^{-1} band relative to that of the 375 cm^{-1} band as a function of waveguide 55 (open boxes) segment number from device U941123.14. The mean value of S_{342}/S_{375} for waveguide 55, excluding segment No. 1, is 0.862 ± 0.017, whereas that for the KTP substrate (X) is 1.14 ± 0.01.

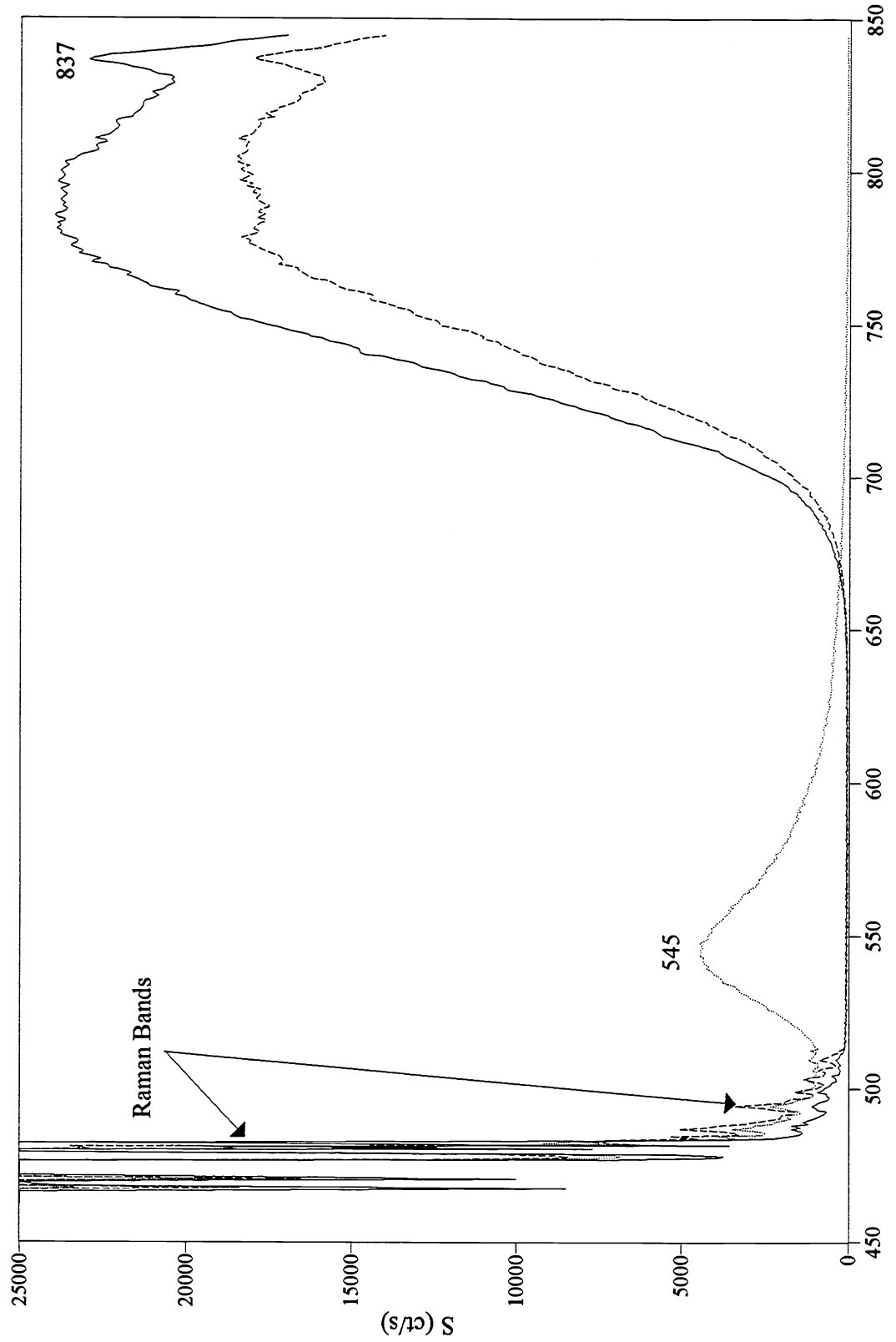

Fig. 6. Laser excited luminescence spectra of KTP substrates from channel waveguide devices IBM R/KTP (solid), S1.3 (dotted), and IBM F11 (dash dot). The excitation wavelength was 457.9 nm.